

Understanding Stokes-Einstein Relation in Supercooled Liquids using Random Pinning

Bhanu Prasad Bhowmik*, Rajsekhar Das* and Smarajit Karmakar†
*Centre for Interdisciplinary Sciences, Tata Institute of Fundamental Research,
 21 Brundavan Colony, Narsingi, Hyderabad, 500075, India*

Breakdown of Stokes-Einstein relation in supercooled liquids is believed to be one of the hallmarks of glass transition. The phenomena is studied in depth over many years to understand the microscopic mechanism without much success. Recently it was found that violation of Stokes-Einstein relation in supercooled liquids can be tuned very systematically by pinning randomly a set of particles in their equilibrium positions. This observation suggested a possible framework where breakdown of Stokes-Einstein relation in the dynamics of supercooled liquids can be studied with precise control. We have done extensive molecular dynamics simulations to understand this phenomena by analyzing the structure of appropriately defined set of dynamically slow and fast particles clusters. We have shown that the Stokes-Einstein breakdown actually become predominant once the cluster formed by the slow particles percolate the entire system size. Finally we proposed a possible close connection between fractal dimensions of these clusters and the exponents associated with the fractional Stokes-Einstein relation.

I. INTRODUCTION

The dynamics of supercooled liquids and associated glass transition where viscosity or relaxation time increases dramatically with decreasing temperature still puzzle the scientific community even after decades of research [1–8]. The viscosity change is so dramatic that with few tens of degrees of change in temperature, viscosity can change as much as 16 orders of magnitude and the temperature at which viscosity reaches 10^{16} Poise is termed the calorimetric glass transition temperature, T_g . There are many interesting features seen in the dynamics of supercooled liquids approaching this calorimetric glass transition that are not observed in normal liquids. One such example is the temporal density-density correlation functions which in the supercooled temperature regime show multiple relaxation steps. The short time relaxation is termed as β -relaxation [9] and the longer time scale relaxation is called α -relaxation as shown in Fig. 1. One of the most puzzling phenomena observed in the long time α -relaxation process is the breakdown of the famous Stokes-Einstein relation [10–12]. This is one of the most studied phenomena in the context of supercooled liquids without a clear general consensus [13–25]. Thus a better understanding of this phenomena will definitely be of immediate importance for developing theory of glass transition.

Stokes-Einstein relation connects viscosity of a liquid (η) to the diffusion constant (D) as

$$D \propto \frac{k_B T}{\eta} \quad (1)$$

where k_B is the Boltzmann constant. The constant of proportionality depends on the details of the probe par-

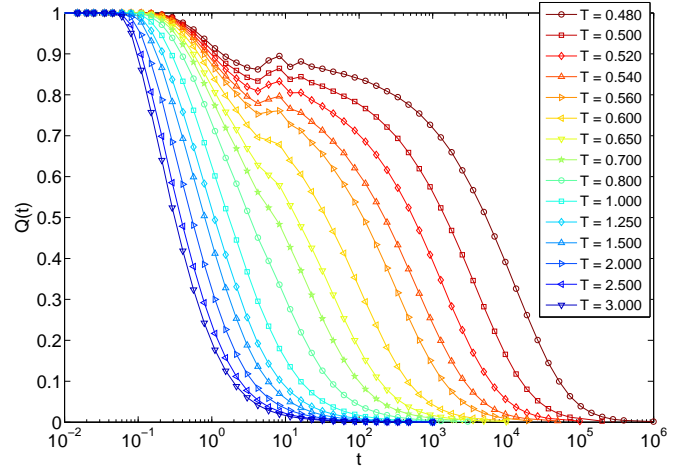


FIG. 1: Two point density-density correlation function $Q(t)$ (see text for definition) obtained from molecular dynamics simulations of a binary glass forming liquids for different temperatures as indicated in the legend. Notice the appearance of two step relaxation with decreasing temperature.

ticles used to measure the diffusion constant of the liquids. One often uses self-diffusion constants instead of tracer diffusion in the above equation for simple liquids interacting via isotropic pairwise potential. It is found that at least in the low temperature regime viscosity, η is proportional to the long time α -relaxation time, τ_α [26] (see method section for definition), so it is customary in the literature to cast the Stokes-Einstein relation in the following form

$$D \propto \frac{k_B T}{\tau_\alpha} \quad (2)$$

where η is replaced by τ_α . The other reason for this modification lies in the fact that calculation of τ_α is much eas-

*These authors contributed equally

†Electronic address: smarajit@tifrh.res.in

ier and straight forward than the viscosity (Notice that it is already shown in the literature that this is not the reason for breakdown in Stokes-Einstein relation). Thus if one plots $D\tau_\alpha/T$ as a function of T , then it should be temperature independent constant, but it turns out that for supercooled liquids this ratio becomes a strong function of temperature below some temperature. Phenomenological arguments [13, 16] often assume existence of dynamic heterogeneity [27–35] which means existence of mobile and less mobile dynamical regions in the supercooled liquid states in order to explain the violation of Stokes-Einstein relation. Many previous studies indeed showed positive correlation between Stokes-Einstein breakdown and Dynamic Heterogeneity [22, 34] as measured by four-point density-density correlation function.

Sometimes a generalized version of the Stokes-Einstein relation [19, 47] is also used to describe the inter-relationship between diffusion constant and relaxation time in the supercooled regime with the following form

$$D \propto \tau_\alpha^{-1+\omega} \quad (3)$$

where exponent ω characterizes the degree of deviation from normal Stokes-Einstein relation. This relation is called fractional Stokes-Einstein relation and in [19, 47], it was shown that fractional Stokes-Einstein exponent can depend on the dimensionality of the system as well as on the details of the microscopic interaction between particles.

From the Mean Field arguments, it is expected that ω will go to zero as one increases the spatial dimensions. This expectation is broadly supported by the results reported in [22, 48–50]. A detailed numerical study on this aspect [49] in a hard sphere glass forming liquids showed that the fractional Stokes-Einstein exponent ω actually goes to zero at eight dimensions. This provided for the first time a direct estimate of the upper critical dimension for glass forming liquids, above which mean field type description of the liquids should hold [49]. One should keep in mind that computational cost increases very rapidly with increasing dimensionality of a system and simulation of any mean field model is actually a very difficult numerical task [22, 49, 50]. Thus it is needless to say that it would be extremely useful if one can change fractional Stokes-Einstein exponent with ease in a model system just by tuning some parameters.

In [51], it was shown that one can change fractional Stokes-Einstein exponent with ease in model systems simply by randomly pinning some fraction of particles in their equilibrium positions [36, 39–46, 52]. Here we will use this protocol to understand in depth the breakdown of Stokes-Einstein relation and its relation with any underlying structural changes in the liquids. The rest of the paper is organized as follows: first we will give details of the model system studied, then will give the definitions of the different dynamical quantities calculated in this study with the details of the pinning protocol used to generate random pinning in the system. Then we will discuss the results obtained and finally discuss implica-

tions of these results on our understanding of breakdown of the Stokes-Einstein relation.

II. METHOD AND SIMULATION DETAILS

Model: We perform simulations for a model glass forming liquids in two dimensions in this work. The model is characterized by a repulsive inverse power-law potential (2dR10) [52]. This model has been studied extensively and found to be a very good glass former. The interaction potential is given by

$$V_{\alpha\beta}(r) = \epsilon_{\alpha\beta} \left(\frac{\sigma_{\alpha\beta}}{r} \right)^n \quad (4)$$

where $\alpha, \beta \in \{A, B\}$ and $\epsilon_{\alpha\beta} = 1.0$, for all α and β . $\sigma_{AA} = 1.0$, $\sigma_{AB} = 1.18$, $\sigma_{BB} = 1.40$, and $n = 10$. The interaction potential was cut off at $1.38\sigma_{\alpha\beta}$. For this model the system sizes studies are $N = 1000$ and $N = 10000$ at a number density $\rho = 0.850$ for many different temperatures in the range $T \in [0.480, 3.000]$. These simulations are done in the canonical ensemble using a modified leap-frog integration scheme with the Berendsen thermostat. We have also performed simulation with another constant temperature simulation algorithm due to Brown and Clark [53]. The results do not depend on the exact algorithm used for integrating the equations of motion. We have averaged the data over 32 independent runs of length 100 τ .

Pinning Protocol: In this study we have pinned some fraction ρ of total number of particles randomly from their equilibrium configurations. First we equilibrate a system of given number of particles, N at the studied temperatures and then we choose randomly $N_p = \rho N$ number of particles from one such equilibrated configuration and pinned their positions. The advantage of such pinning protocol is that the system with the pinned particles are already in equilibrium as the positions of the pinned particles are taken from an equilibrium configurations. This procedure bypasses re-equilibration of the system after introducing these form of quenched disorder. We then do averaging over the different realizations of these pinning positions (averaging over quenched disorder) to calculate different thermodynamic and dynamic quantities. In this study we have done averaging of 32 different realizations of disorder and we checked that this amount of averaging is enough to get reliable results. One can also pin particles in an ordered arrangements with further equilibration and results may depend on the details of the pinning protocol but we don't expect much qualitative change in the reported results.

Correlation Functions: Dynamic heterogeneity in the system is characterized by the four-point density cor-

relation function $g_4(r, t)$ [54–56] defined as

$$g_4(\mathbf{r}, t) = [\langle \delta\rho(0, 0)\delta\rho(0, t)\delta\rho(\mathbf{r}, 0)\delta\rho(\mathbf{r}, t) \rangle] - [\langle \delta\rho(0, 0)\delta\rho(0, t) \rangle][\langle \delta\rho(\mathbf{r}, 0)\delta\rho(\mathbf{r}, t) \rangle] \quad (5)$$

where $\delta\rho(\mathbf{r}, t)$ represents the deviation of the local density at point \mathbf{r} at time t from its average value, and $\langle \dots \rangle$ represents a thermal or time average and $[\dots]$ represents quenched disorder average. This function quantifies the correlation of the relaxation of density fluctuations at two points separated by distance r . A four-point susceptibility may be defined as the $k = 0$ value of the Fourier transform $g_4(\mathbf{k}, t)$ of this function. A variant [57] of this four-point function has been used extensively in numerical studies of dynamic heterogeneity because it is easier to compute. This quantity is obtained from the overlap function $q(t)$ defined as

$$q(t) = \frac{1}{N - N_p} \sum_{i=1}^{N-N_p} w(|\mathbf{r}_i(0) - \mathbf{r}_i(t)|), \quad (6)$$

where $\mathbf{r}_i(t)$ is the position of particle i at time t , N is the total number of particles and N_p is the number of pinned particles. $w(r) = 1$ if $r \leq a_0$ and zero otherwise, and a_0 is a short-distance cutoff chosen to be close to the distance at which the root-mean-square displacement of the particles as a function of time exhibits a plateau (the precise choice of the value of a_0 turns out to be qualitatively unimportant). This function may be viewed as the “self” part of the density correlation function

$$C(t) = \int d\mathbf{r} \rho(\mathbf{r}, 0)\rho(\mathbf{r}, t), \quad (7)$$

with the window function $w(r)$ used to treat particle positions separated by distances smaller than a_0 , due to small-amplitude vibrational motion in the “cage” formed by neighboring particles, to be the same. The thermal averaged and disorder averaged overlap function $Q(t) = [\langle q(t) \rangle]$. The fluctuations in this two point function yields the dynamical four-point susceptibility:

$$\chi_4(t) = \frac{1}{N - N_p} \left([\langle q^2(t) \rangle] - [\langle q(t) \rangle]^2 \right). \quad (8)$$

with the peak value defined as $\chi_4^P \equiv \chi_4(t = \tau_4)$, where τ_4 is the time at which $\chi_4(t)$ attains its maximum value and $\tau_4 \simeq \tau_\alpha$ at all temperatures. The α -relaxation time τ_α is defined using the two-point correlation function as $Q(t = \tau_\alpha) = 1/e$.

Diffusion Constant: The diffusion constant D for different temperatures and pinning density is calculated from the slope of the mean squared displacement using the relation

$$\langle \Delta r^2(t) \rangle = 2dDt \quad (9)$$

where d is the spatial dimension and in this case $d = 2$.

van Hove function: van Hove function, $G(x, t)$ is the probability of finding a displacement of a particle of amount x over a timescale of t . It is formally defined as follows

$$G(x, t) = \sum_{i,j=1}^N \delta(x - x_i(t) - x_j(0)) \quad (10)$$

where $x_i(t)$ is one of the coordinates of the position of particle i at time t and the self part of this correlation function is defined as

$$G_s(x, t) = \sum_{i=1}^N \delta(x - x_i(t) - x_i(0)) \quad (11)$$

Here we have calculated only self part of the van Hove correlation function for simplicity.

III. RESULTS

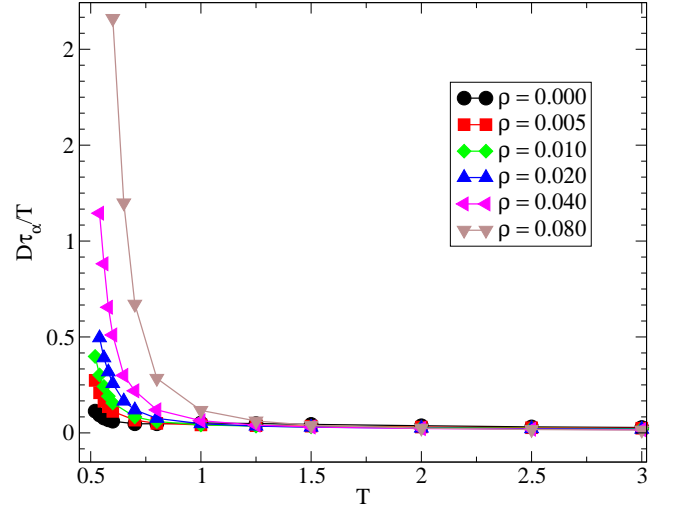


FIG. 2: The Stokes-Einstein parameter $D\tau_\alpha/T$ is plotted as a function of temperature for different pinning concentration, ρ . One can clearly see that at high temperatures the parameter is almost independent of temperature and starts to become temperature dependent somewhat sharply. The temperature at which the breakdown happens increases to higher value with increasing pinning concentration.

In Fig.2, we have plotted the Stokes-Einstein parameter $D\tau_\alpha/T$ as a function of temperature for different pinning density. One can clearly see that the quantity is fairly independent of temperature up to some temperature for a given pinning concentration and then it start to increase, indicating the violation of Stokes-Einstein relation in these temperature regimes. The phenomena becomes even more prominent with increasing pinning concentration and the Stokes-Einstein parameter becomes strongly temperature dependent and the temperature at

which this violation happens seems to also increase with increasing pinning concentration as shown in Fig.2. Thus pinning a set of randomly chosen particles in their equilibrium positions will be an excellent model system to understand breakdown of Stokes-Einstein relation in supercooled liquids.

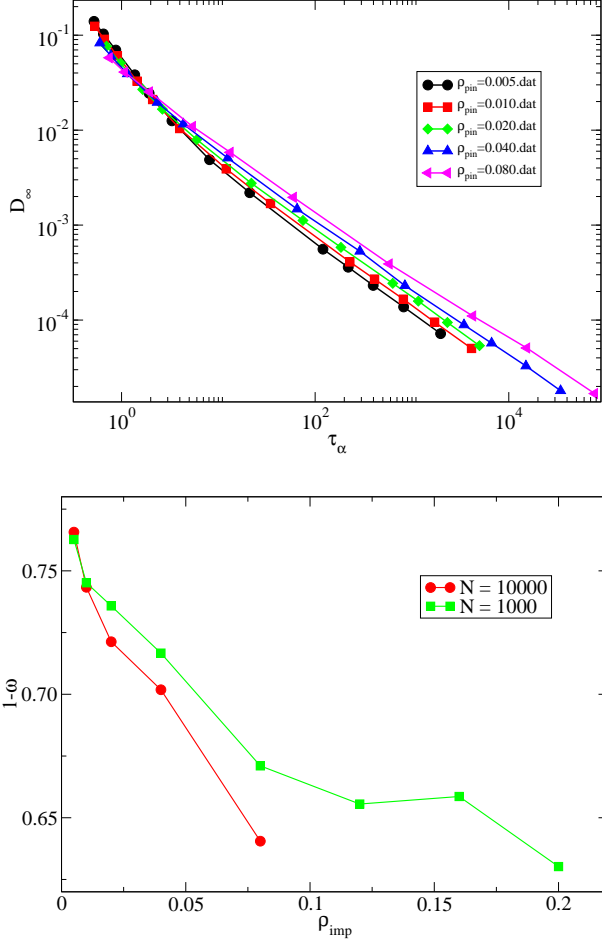


FIG. 3: Top panel: Fractional Stokes-Einstein relation, τ_α is plotted as function of D for different pinning concentrations and one can see that at higher temperature $D \sim 1/\tau_\alpha$, but at lower temperatures this relation breaks down and one gets $D \sim \tau_\alpha^{-1+\omega}$ with $\omega > 0$. This exponent seems to increase with increasing pinning concentration as shown in the Bottom panel. Note that ω seems to significant finite size effect and increases faster with increasing pinning concentration for $N = 10000$ system size.

In the same context it is important to discuss the fractional Stokes-Einstein relation and how the exponent depends on the pinning density. In Fig.3, we have plotted D vs τ_α in log-log plot for different pinning density. As in [51], we have found that at higher temperatures $D \propto \tau_\alpha^{-1}$, but as one goes to lower temperature, this relation breaks down and one gets $D \propto \tau_\alpha^{-1+\omega}$, with $\omega > 0$. The value of the fractional Stokes-Einstein exponent ω increases continuously with increasing pinning density as

shown in lower panel of Fig.3. These observations also give us an opportunity to gain better understanding of the phenomena without much computational difficulty. For the rest of the paper we will discuss about the correlation between different dynamical measures of Dynamic Heterogeneity and their correlation with the breakdown of Stokes-Einstein relation.

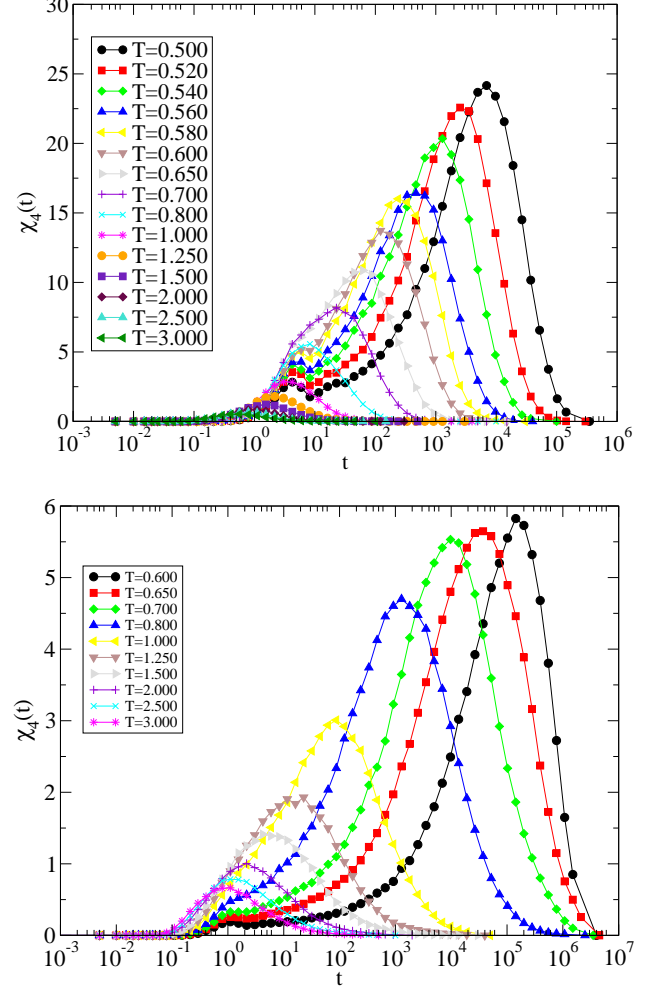


FIG. 4: Top panel: Four-point dynamic susceptibility, $\chi_4(t)$ as a function of time for different temperatures. Notice the monotonic increase in the peak height of $\chi_4(t)$ with decreasing temperature. This is for pinning concentration, $\rho = 0.020$. Bottom panel: Similar plot but for higher pinning concentration $\rho = 0.120$. Notice although the peak height increases monotonically the absolute value of this function is many times smaller than the $\rho = 0.020$ case.

As discussed before many phenomenological theories suggest Stokes-Einstein breakdown to be due to the presence of dynamic heterogeneity in the system at the supercooled temperature regime [16, 22] and indeed some correlation was also found in [22]. It was found that peak height of χ_4 starts to grow rapidly at a temperature very close to the temperature where Stokes-Einstein breakdown seems to happen for different model system in

different dimensions. To see whether similar correlation exists here for the pinned system, we have calculated the four-point susceptibility as shown in different panels of Fig.4. One can see the usual temperature dependence of $\chi_4(t)$ for different pinning density ρ .

It is interesting to note that actual peak height of $\chi_4(t)$ decreases with increasing pinning density as can be seen in top panel of Fig.5, where temperature dependence of χ_4^P is plotted for different pinning density and one sees that χ_4^P decrease with increasing pinning density. It becomes much clearer when χ_4^P is plotted as a function of pinning density for different temperature as shown in the bottom panel of the same figure. This clearly shows that χ_4^P completely fails to capture Stokes-Einstein breakdown for these model system. Actually it shows anti-correlation.

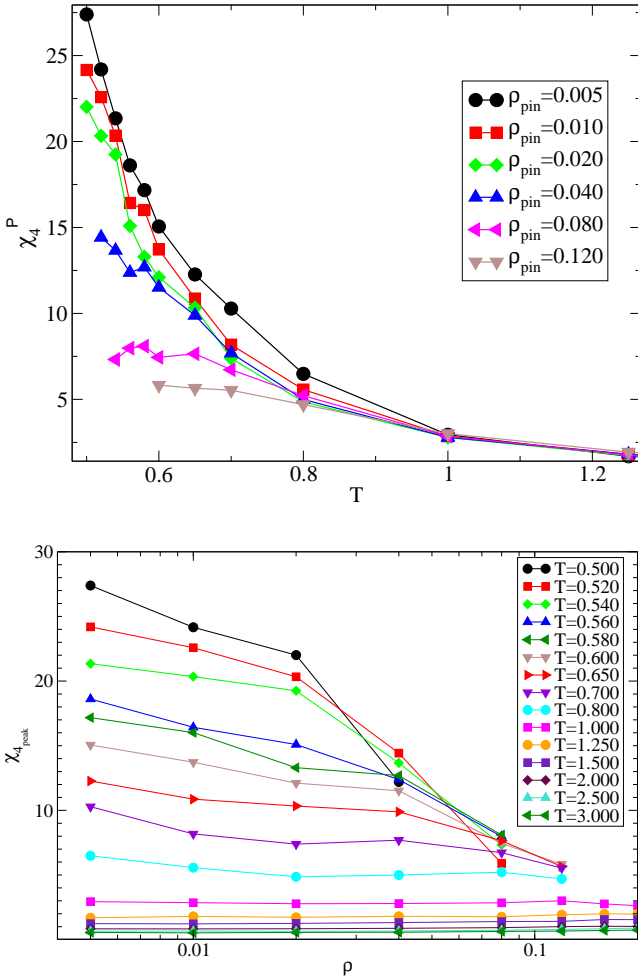


FIG. 5: Top panel: Peak height of $\chi_4(t)$, χ_4^P as a function of temperature for pinning concentration. Notice that temperature dependence of χ_4^P become much more weak with increasing pinning concentration. Bottom panel: χ_4^P as a function of pinning concentration for different temperatures.

Next we check whether the exponent β , related to stretched exponential decay of two-point correlation

function is correlated with the Stokes-Einstein breakdown as found in [22]. We followed the similar fitting procedure as described in [22], to get the exponent β by fitting the $Q(t)$ data to the following fitting function

$$Q(t) = A \exp \left[-\left(\frac{t}{\tau_1} \right)^2 \right] + B \exp \left[-\left(\frac{t}{\tau_\alpha} \right)^\beta \right] \quad (12)$$

Although it is a non-linear fitting with 5 parameters,

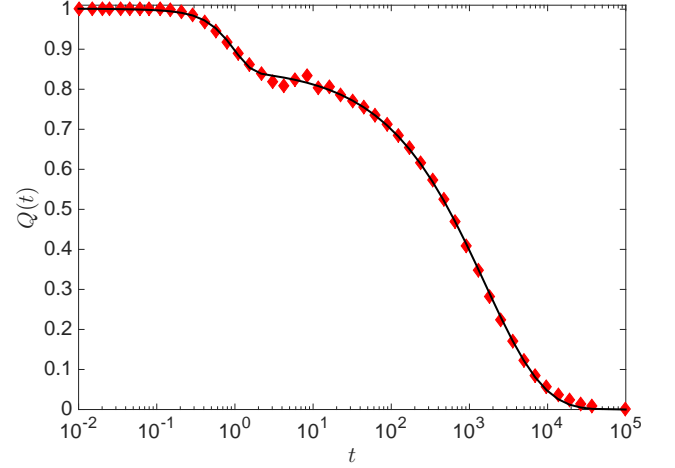


FIG. 6: Fitting of $Q(t)$ using Eq.12 for temperature $T = 0.520$ and $\rho = 0$. The fitting observed is very good over the whole time window and thus one can be confident of the obtained values of stretched exponent β .

with good initial choice of the parameters the fitting converges to the right solution very quickly without any problem as can be seen in Fig.6. The quality of the fit gives us the confidence on the reliability of the extracted values of the exponent β .

In Fig.7, we have shown the stretched exponent β as a function of temperature for different pinning density and one can clearly see that β becomes smaller and smaller with increasing pinning density. In [22], it was shown that β becomes closer to one as one increases dimensions of the system from $d = 2$ to $d = 4$ and Stokes-Einstein breakdown also becomes less prominent with increasing dimensionality. Thus it seems stretched exponent β to be an excellent identifier of the Stokes-Einstein breakdown even for the pinned systems.

Now if we assume that stretched exponential relaxation is related to hierarchical relaxation processes, then one can write

$$Q(t) \sim \exp(-t/\tau_\alpha)^\beta = \int_0^\infty P(\tau) \exp(-t/\tau) d\tau \quad (13)$$

where β will be related to the relative variance of the distribution and smaller β will corresponds to larger relative width of the distribution. To ascertain that we have discretized the above equation to calculate the distribution

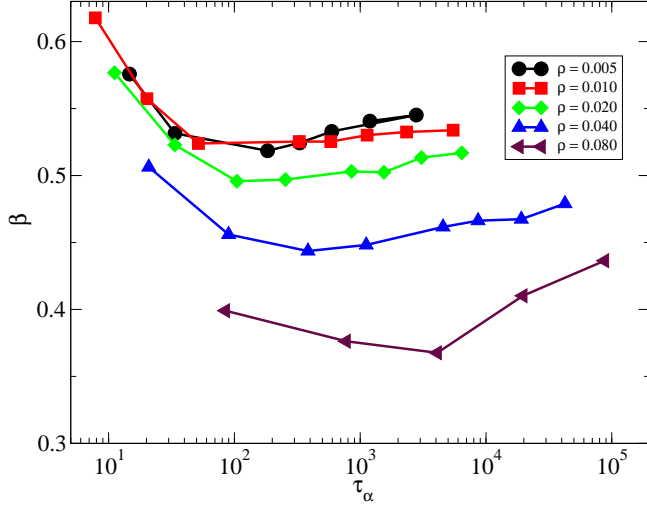


FIG. 7: Stretched exponent β as a function of α -relaxation time scale τ_α for different pinning concentrations. Notice that β becomes significantly smaller for larger pinning concentration at lower temperature.

$P(\tau)$ by minimizing χ^2 ,

$$\chi^2 = \sum_{i=1}^m \left[Q(t_i) - \sum_{j=1}^M P_j \exp(-t_i/\tau_j) \Delta\tau \right]^2 \quad (14)$$

where m is the number of time points t_i , where two point-correlation function $Q(t)$ is obtained from simulations and M is the number of discretized τ values (τ_j) where we want to find out the probability density P_j . $\Delta\tau = \tau_{j+1} - \tau_j$, is the elementary discretization step size. One crucial transformation which is required to get the required convergence of the χ^2 minimization is to do the following variable change, $P_j = p_j^2$ and then minimize with respect to the new variable p_j . This ensures the positivity of the probability [58]. As shown in top panel of Fig.8, the convergence is quite good and one can get very reliable estimate of the underlying probability distribution of the relaxation time. We have calculated the probability for all the different temperatures at different pinning density but showing the results for three different pinning concentrations at temperatures where τ_α are comparable to each other. The results clearly show that indeed the normalized distribution tends to have fatter tail in the larger τ values with increasing pinning density. The nice bi-modality of the distribution is also interesting and will discuss this issue in the context of distribution of diffusion constants.

Still now we have shown that peak height of $\chi_4(t)$ does not seem to capture the increasing degree of Stokes-Einstein violation in the pinned system, whereas stretched exponent β and the associated distribution of relaxation time seem to correlate very well. Next we will quantify the dynamic heterogeneity by identifying "slow" and "fast" particles over the α -relaxation time scale as

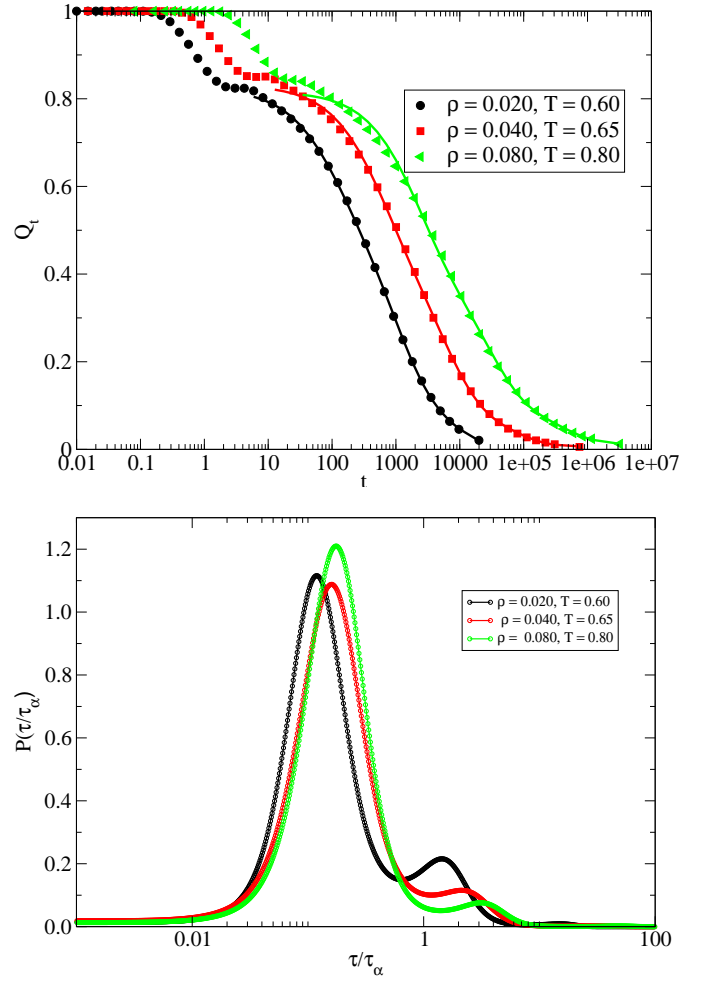


FIG. 8: Top panel: Convergence of χ^2 -optimization, Eq.14. Time axes of $Q(t)$ for $T = 0.65, \rho = 0.040$ and $T = 0.80, \rho = 0.080$ are multiplied by 3 and 8 respectively for the clarity. Bottom panel: The obtained distribution of relaxation time, $P(\tau)$. The probabilities for different pinning concentrations and temperatures are plotted after rescaling the timescale by τ_α for better comparison. Notice that distribution gets fatter and fatter for larger values of τ with increasing pinning concentration, completely consistent with exponent β being smaller in the respective cases.

done in [51] and show the results on the clustering properties of these slow particles in the system to elucidate their role in breakdown of Stokes-Einstein relation.

We will first briefly discuss the method used to obtain the distribution of diffusion constants from the van Hove correlation function using Lucy iteration [59]. This method is also recently used in [60] for the diffusion processes in biological systems. We start with the following assumption: that particles' displacements are mainly caused by diffusion processes. Due to dynamic heterogeneity in the system at least in the supercooled temperature regime it is not very surprising to expect that there will be a distribution of local diffusivity $p(D)$. Then we

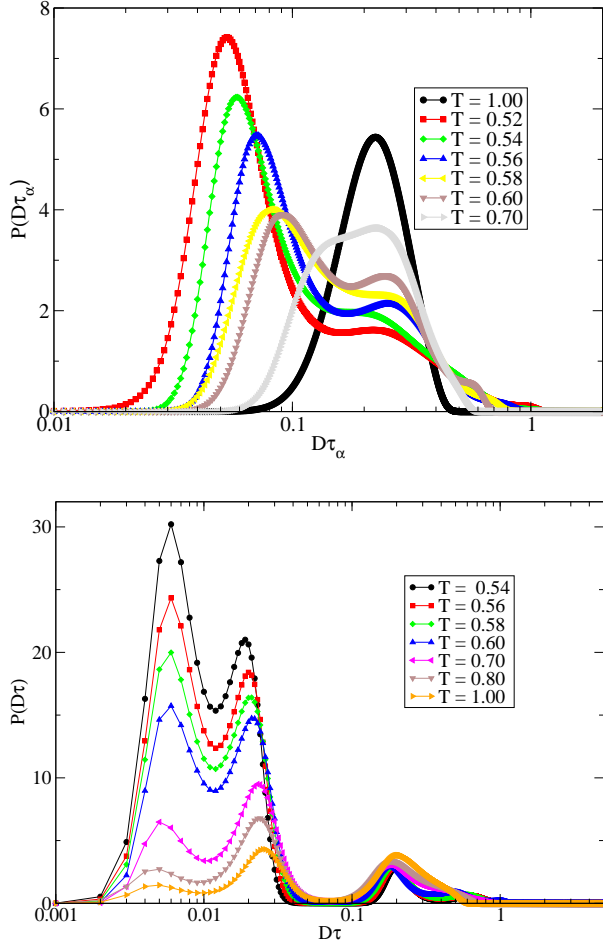


FIG. 9: Distribution of diffusion constants for different temperatures for $\rho = 0.00$ (top panel) and $\rho = 0.020$ (bottom panel). Notice the bimodal distribution at lower temperatures.

can express van Hove correlation function calculated at α -relaxation timescale, $G_s(x, \tau_\alpha)$ in terms of $p(D)$ as

$$G_s(x, \tau_\alpha) = \int_0^{D_0} p(D) \cdot g(x|D) \cdot dD, \quad (15)$$

where $g(x|D) = 1/\sqrt{4\pi D\tau_\alpha} \exp(-x^2/4D\tau_\alpha)$ and D_0 is the upper limit of diffusion constant and will be equal to diffusivity for a free diffusion. Now given the $G_s(x, \tau_\alpha)$ we calculate the distribution of diffusivity $p(D)$ following [59] as

$$p^{n+1}(D) = p^n(D) \int_{-\infty}^{\infty} \frac{G_s(x, \tau_\alpha)}{G_s^n(x, \tau_\alpha)} g(x|D) dx, \quad (16)$$

where $p^n(D)$ is the estimate of $p(D)$ in the n^{th} iteration with $p^0(D) = (1/D_{avg}) \exp(-D/D_{avg})$ and

$$G_s^n(x, \tau_\alpha) = \int_0^{D_0} p^n(D) \cdot g(x|D) \cdot dD. \quad (17)$$

Similarly

$$P^{n+1}(D\tau_\alpha) = P^n(D\tau_\alpha) \int_{-\infty}^{\infty} \frac{G_s(x, \tau_\alpha)}{G_s^n(x, \tau_\alpha)} g(x|D) dx, \quad (18)$$

where $p(D)dD = P(D\tau_\alpha)d(D\tau_\alpha)$. The choice of $D\tau_\alpha$ as our variable is due to the fact that D changes by several orders of magnitude in the studied temperature range whereas $D\tau_\alpha$ changes relatively modestly with decreasing temperature and it will be easier to compare the distribution obtained for different temperatures (Please see [51] for further details).

In Fig.9, we have shown the obtained distribution of diffusion constants for different pinning concentrations. For the unpinning case the distribution is very nicely bimodal below some temperatures, clearly telling us that one can easily identify a set of "slow" and "fast" moving particles over α -relaxation time scale. Notice that at much larger time than τ_α the dynamic heterogeneity will be averaged out and one expects the corresponding van Hove function to become Gaussian. Thus at longer timescale the distribution will also lose its bimodality, but as already shown in [51], the bimodal feature remains intact even for timescale which are at least couple of time larger than the α -relaxation timescale. Thus we believe that the results reported here to be qualitatively valid even for timescale larger than the typical relaxation time.

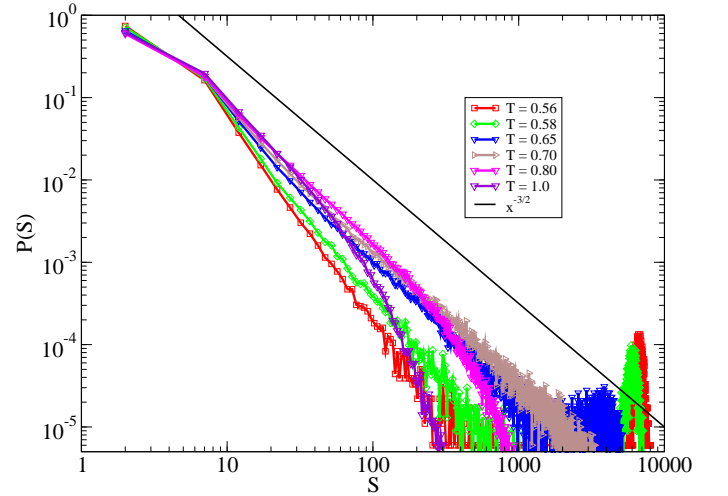


FIG. 10: Distribution of cluster size, $P(S)$ for different temperatures for $\rho = 0.040$. Notice the development of nice power law regime at lower temperatures with slope $-3/2$. At still lower temperatures one can see appearance of a extra hump at larger cluster sizes. This corresponds to system spanning clusters (see text for details).

The cutoff we chose to define such set of particles is the minimum of the two peaks of the bimodal distribution. For system with pinning, the peak associated with the "slow" particles in the distribution splits into two

peaks. This can be understood as follows: with increasing pinning density the difference in the diffusion constants between "slow" and "fast" particles will increase strongly and there will be a set of particles who reside on the boundary of "slow" moving and "fast" moving particles with intermediate diffusion constants. The split of the first peak in $P(D\tau_\alpha)$ we believe is due to these set of particles which becomes prominent with increasing difference in diffusivity between "slow" and "fast" particles. In our studies we have considered the particles with these intermediate diffusion constants to be part of the "slow" particles. As mentioned before, $P(\tau)$ also shows bimodality and it will be interesting to see whether different peaks in that distribution actually correspond to relaxation of "slow" or "fast" moving particles.

Next we have defined a cutoff distance $r_c = \sqrt{4D_c\tau_\alpha}$ at the minimum of the two peaks of the $P(D\tau_\alpha)$ distribution for a given temperature and pinning density. With this definition we define a particles "slow" if it has not moved a distance bigger than the critical distance over τ_α timescale and the others who have move beyond are termed as "fast" particles. In Fig.10, we have plotted the distribution of cluster size for "slow" moving particles for different temperature at pinning concentration $\rho = 0.040$. One can see the appearance of power law distribution at lower temperatures with exponent $P(S) \sim S^{-3/2}$. At still further lower temperatures one can see an appearance of a small hump at larger cluster size, indicating the existence of system spanning cluster. Motivated by this observation we then have tried to study a possible underlying percolation transition associated with the clusters of "slow" moving particles.

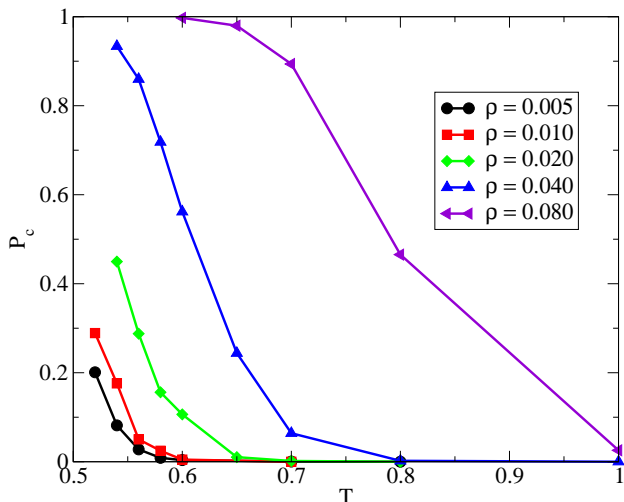


FIG. 11: Probability of finding system spanning cluster of $N = 10000$ as a function temperature for different pinning concentrations. Notice the sharp change in probability at some critical temperature which changes to higher temperatures with increasing pinning concentrations.

In Fig.11, we have plotted the probability of finding

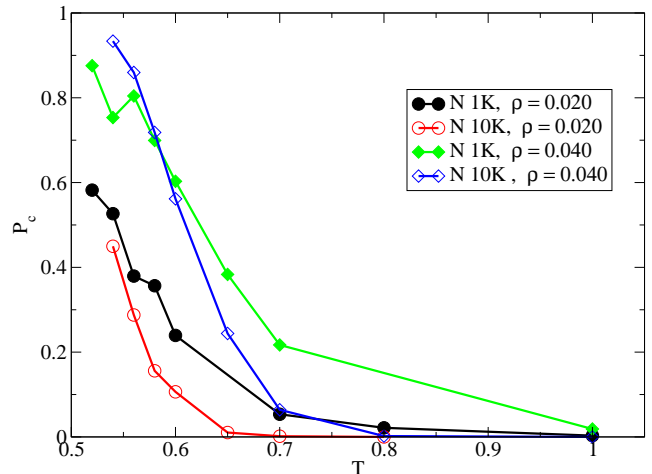


FIG. 12: Probability of finding system spanning cluster, P_c is plotted for two different system sizes $N = 1000$ and $N = 10000$ for two different pinning concentrations. It is clear that growth of P_c for $N = 10000$ system size is much more steeper than $N = 1000$ system, in complete agreement with an underlying percolation transition.

a system spanning cluster, P_c as a function of temperature for different pinning concentration. It is clear that probability of finding system spanning cluster seems to grow sharply after a particular critical temperature and this temperature also shifts to higher values with increasing pinning concentration. Thus we have a clear one to one correspondence between onset of Stokes-Einstein violation and the appearance of system spanning cluster. To establish a clear percolation transition one needs to perform a detailed finite size scaling analysis which we have not yet performed here in this study due to large computational requirements.

We also have studied the phenomena for another system size with $N = 1000$ particles. For percolation transition one expects to have a somewhat smoother increase of probability of finding system spanning cluster with decreasing temperature due to finite size effects. In Fig.12, we have plotted P_c as a function of temperature for two different system sizes $N = 1000$ and $N = 10000$ for different pinning concentrations. One can clearly see that P_c increases somewhat less sharply with decreasing temperature for smaller system sizes. Thus confirming a possible underlying percolation transition [61] associated with Stokes-Einstein violation. It will be interesting to perform a detailed finite size scaling analysis to calculate the exponents related to this transition and its connection to slowing down in dynamics in supercooled liquids.

Next we have calculated the mean cluster size as a function of temperature for different pinning concentrations as another indicator of dynamic heterogeneity. As shown in Fig.13, the growth of the mean cluster size is very dramatic and the growth is even more dramatic

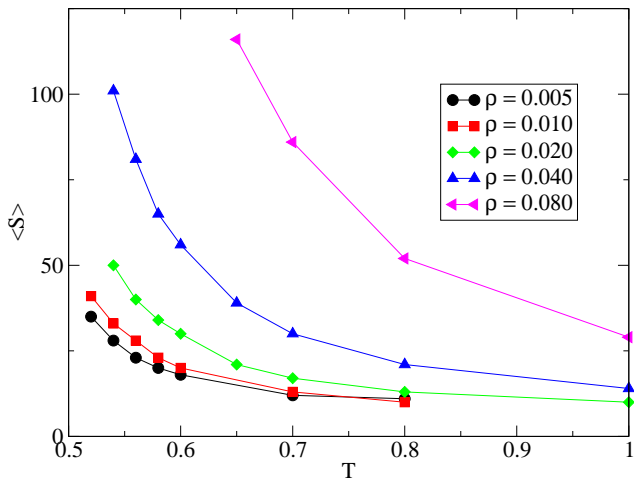


FIG. 13: Temperature dependence of mean cluster size $\langle S \rangle$ for different pinning concentrations. $\langle S \rangle$ shows much stronger temperature dependence with increasing pinning strength, thus confirming growth of Dynamic Heterogeneity in the system.

for higher pinning concentrations, suggesting that indeed dynamic heterogeneity increases with increasing pinning concentration.

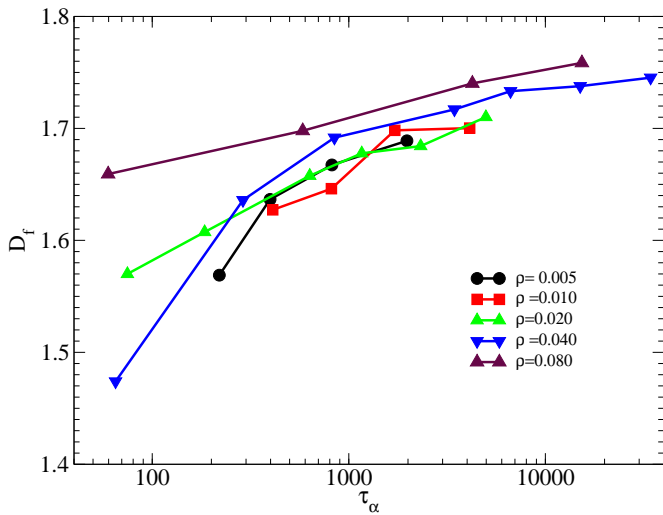


FIG. 14: Fractal dimension of spanning cluster, D_f as a function of temperature for different pinning concentrations. The fractal dimension is systematically larger for system with larger pinning concentrations (see text for detailed discussion).

Finally to understand the origin of fractional Stokes-Einstein exponent, ω , we have calculated the fractal dimensions of these spanning cluster as shown in Fig.14. We have used Sandbox method for determining the fractal dimension of these percolating clusters [62]. It is clear that the clusters are not compact and the fractal dimen-

sions are in the range $D_f \in [1.5-1.8]$ at different temperatures and pinning concentrations. The important thing to notice is that the fractal dimension is systematically larger for the system with increasing pinning concentrations. Thus it seems there is a positive correlation between fractal dimensions of the system spanning cluster and the fractional Stokes-Einstein exponent. Right now we do not have a very clear understanding about this correlation but the following simple arguments seem to suggest such correlation. At higher temperatures $D \sim 1/\tau_\alpha$ and then at lower temperatures $D \sim 1/\tau_\alpha^{1-\omega}$ with $\omega > 0$, which implies that τ_α increases much faster than the rate at which D decreases. This difference in change of τ_α and D with decreasing temperature will be much more prominent if the cluster forms by the "slow" moving particles become more compact. This is due to the fact that τ_α is mainly determined by the relaxation of the "slow" particles and breaking a compact "slow" cluster will be more difficult than breaking a less compact cluster. On the other hand, D is predominantly determined by the diffusion constants of the "fast" moving particles. It will be interesting to see whether such an argument works for system where breaking "slow" particles cluster is even more difficult due to bond formation, for example in the "patchy" colloidal system.

IV. DISCUSSION

To conclude we have performed extensive computer simulations of a model two dimensional glass forming liquids to understand the breakdown of Stokes-Einstein relation in these systems. We found that if one randomly pins some fraction of particles in the system in their equilibrium positions then degree of Stokes-Einstein violation increases dramatically. This enabled us to study Stokes-Einstein violation in supercooled liquids in a systematic manner and also provided us with a model system where exponent related to fractional Stokes-Einstein relation can be tuned very precisely.

Our main findings can be summarized as follows:

- Breakdown of Stokes-Einstein relation in supercooled liquids get enhanced with randomly pinning some fraction of particles in the system and exponent associated with fractional Stokes-Einstein relation also systematically increases with increasing pinning concentration.
- Peak height of $\chi_4(t)$ does not seem to be correlated with Stokes-Einstein breakdown in disagreement with previously reported results.
- The exponent β related to stretched exponential decay of the two point density-density correlation function clearly shows strong correlation with the Stokes-Einstein breakdown in complete agreement with previous studies.

- Appropriately defined "slow" moving particles over α -relaxation timescale seem to form clusters with decreasing temperature and at round the temperature where Stokes-Einstein relation starts to violate, the cluster of "slow" moving particles percolates the whole system size. This indicates a possible deep connection between percolation transition of the "slow" particles and Stokes-Einstein breakdown.
- Mean cluster sizes of "slow" particles in the system grows with decreasing temperature and the growth is much stronger for system with larger pinning concentration.
- The clusters of "slow" particles are fractal like objects with fractal dimensions D_f in the range 1.5 to 1.8 and fractal dimension increases systematically with increasing pinning concentration. Thus there is a positive correlation between fractal dimensions of these clusters with the exponent related to fractional Stokes-Einstein relation. It will be nice to

further understand this correlation in other model glass forming liquids too.

The results reported in this study is only for a model two dimensional system, so it will be interesting to see whether these results hold for three dimensional model system also. It is important to mention here that there are recent studies which seem to suggest a qualitative difference in glass transition in two and three dimensions [63]. Although we don't expect the results reported here to be qualitatively very different even for three dimensional systems but a detailed study is certainly necessary.

V. ACKNOWLEDGMENT

We would like to thank Kunimasa Miyazaki and Jürgen Horbach for many useful discussions. Kallol Paul and Indrajit Tah are acknowledged for critical reading of the manuscript and discussions.

-
- [1] Debenedetti P 1997 *Metastable Liquids* (Princeton University Press, Princeton, New Jersey)
 - [2] S.P. Das, Rev. Mod. Phys. **76**, 785 (2004).
 - [3] Berthier L and Biroli G 2011 *Rev. Mod. Phys.* **83** 587
 - [4] V. Lubchenko and P. G. Wolynes, Annu. Rev. Phys. Chem. **58**, 235 (2007).
 - [5] F. Ritort and P. Sollich, Adv. Phys. **52**, 219 (2003).
 - [6] D. Chandler *et al.*, *Phys. Rev. E* **74**, 051501 (2006).
 - [7] S. Karmakar, C. Dasgupta and S. Sastry, Annu. Rev. Condens. Matter Phys. **5**, 255 (2014).
 - [8] S. Karmakar, C. Dasgupta and S. Sastry, Report. on Progress in Physics **79**, 016601 (2015).
 - [9] S. Karmakar, C. Dasgupta and S. Sastry, *Short-time β -relaxation in glass-forming liquids is cooperative in nature*, arXiv:1506.08074 (2015).
 - [10] J. Hansen and I. R. McDonald, Theory of Simple Liquids (3rd Ed.), Elsevier (2008).
 - [11] A. Einstein, Ann. Phys. **17**, 549 (1905); English translation: A. Einstein, Investigations on the theory of the Brownian movement, Dover, NY (1956).
 - [12] L. D. Landau and E. M. Lifshitz, Fluid Mechanics, 2nd. Ed., Pergamon Press (1987).
 - [13] J. A. Hodgdon and F. H. Stillinger, *Phys. Rev. E*, **48**, 207 (1993); F. H. Stillinger and J. A. Hodgdon, *Phys. Rev. E*, **50**, 2064 (1994).
 - [14] I. Chang and H. Sillescu, *J. Phys. Chem. B*, **101**, 8794 (1997).
 - [15] W. Kob and H. C. Andersen, Phys. Rev. Lett., **73**, 1376 (1994).
 - [16] G. Tarjus and D. Kivelson, J. Chem. Phys., **103**, 3071 (1995).
 - [17] G. Monaco, D. Fioretto, L. Comez and G. Ruocco, Phys. Rev. E, **63**, 061502, (2001).
 - [18] S. Chen *et al.*, *Proc. Natl. Acad. Sci. (US)*, **103**, 12974 (2006).
 - [19] S. Becker, P. Poole, F. Starr, *Phys. Rev. Lett.*, **97**, 055901, (2006).
 - [20] F. Mallamace *et al.*, *J. Phys. Chem. B*, **114**, 1870, (2010).
 - [21] E. La Nave, S. Sastry and F. Sciortino, *Phys. Rev. E*, **74**, 050501(R) (2006).
 - [22] S. Sengupta, S. Karmakar, C. Dasgupta and S. Sastry, The Journal of chemical physics **138** (12), 12A548 (2013).
 - [23] L. Xu *et al.*, *Nature Physics*, **5**, 565, (2009).
 - [24] M. D. Ediger, *Annu. Rev. Phys. Chem.* **51**, 99 (2000).
 - [25] C. De Michele and D. Leporini, *Phys. Rev. E* **63** 036701 (2001).
 - [26] Z. Shi, P/G. Debenedetti, and F.H. Stillinger. J. Chem. Phys. **138**, 12A526 (2013).
 - [27] M. D. Ediger, Annu. Rev. Phys. Chem. **51**, 99 (2000).
 - [28] R. Yamamoto and A. Onuki, J. Phys. Soc. Jpn. **66**, 2545 (1997).
 - [29] M. M. Hurley and P. Harrowell, Phys. Rev. E **52**, 1694 (1995).
 - [30] C. Donati, *et al.*, Phys. Rev. Lett. **80**, 2338 (1998).
 - [31] W. K. Kegel and A. van Blaaderen, *Science*, **287**, 290 (2000); E. R. Weeks, J.C. Crocker, A. C. Levitt, A. Schoeld and D.A. Weitz, *Science*, **287**, 627 (2000); A. Widmer-Cooper, H. Perry, P. Harrowell and D. R. Reichman, *Nat. Phys.*, **4**, 711, (2008).
 - [32] S. Karmakar, C. Dasgupta, and S. Sastry, Proc. Nat. Acad. Sci. (USA) **106**, 3675 (2009).
 - [33] S. Karmakar, C. Dasgupta, and S. Sastry, Phys. Rev. Lett. **105**, 015701 (2010).
 - [34] S. Kumar, G. Szamel and J.F. Douglas J. Chem. Phys. **124**, 214501 (2006).
 - [35] P. Chaudhuri, L. Berthier and W. Kob, Phys. Rev. Lett. **99**, 060604 (2007).
 - [36] K. Kim, Europhys Lett **61**:79095 (2003).
 - [37] S. Karmakar, E. Lerner and I. Procaccia Physica A, **391**, 1001 (2012).
 - [38] S. Karmakar, G. Parisi, Proc. Nat. Acad. Sci. **110**, 2752 - 2757 (2013).

- [39] L. Berthier, W. Kob, Phys Rev E **85**: 011102-1 011102-5 (2012).
- [40] W. Kob and L. Berthier, Phys. Rev. Lett. **110**, 245702 (2013).
- [41] C. Cammarota and G. Biroli, Proc. Nat'l. Acad. Sci. USA **109**:8850-8855 (2012).
- [42] K. Kim, K. Miyazaki, S. Saito, J Phys: Condens Mat **23**:234123 (2011).
- [43] V. Krakoviack, Phys. Rev. E **84**, 050501(R) (2011).
- [44] G. Szamel and E. Flenner, Euro. Phys. Lett. **101**, 66005 (2013).
- [45] S. Chakarabarty, S. Karmakar and C. Dasgupta, Scientific Reports **5**, 12577 (2015).
- [46] S. Chakarabarty, S. Karmakar and C. Dasgupta, Proc. Natl. Acad. Sci. **112** (35) E4819-E4820 (2015).
- [47] J.F. DOUGLAS and D. LEPORINI, *J. Non-Cryst. Solids*, **235**, 137 (1998).
- [48] P. Charbonneau, A. Ikeda, J. A. van Meel, and K. Miyazaki, *Phys. Rev. E*, **81**, 040501 (R), (2010).
- [49] P. Charbonneau, G. Parisi and F. Zamponi, arXiv:1210.6073
- [50] J. D. Eaves and D. R. Reichmann, Proc. Natl. Acad. Sci. (US), **106**, 15171, (2009).
- [51] S. Sengupta and S. Karmakar, The Journal of chemical physics **140** (22), 224505 (2014).
- [52] S. Karmakar, E. Lerner, I. Procaccia and and Jacques Zylberg Phys. Rev. E **82** 031301 (2010).
- [53] D. Brown and J.H.R. Clark, Mol. Phys. **51**, 1243 (1984).
- [54] C. Dasgupta, *et al.*, Europhys. Lett. **15**, 307 (1991).
- [55] S. Franz and G. Parisi, J. Phys. Condens. Matter **12**, 6335 (2000).
- [56] C. Donati, *et al.*, J. Non-Cryst. Sol. **307-310**, 215 (2002).
- [57] Lacevic N, Starr F W, Schroder T B, Novikov V N and Glotzer S C 2002 *Phys. Rev. E* **66** 030101(R)
- [58] C. Dasgupta 1992 Europhysics Lett. **20** 131 (1992).
- [59] L.B. Lucy Astron. J. **79**, 745 (1974).
- [60] B. Wang, J. Kuo, S.C. Bae and S. Granick, Nat. Mat. **11**, 481 (2012).
- [61] D. Stauffer and A. Aharony, *Introduction to Percolation Theory*, Taylor & Francis, (1994).
- [62] T. Tél, A. Fülöp, and T. Vicsek, Physica A **159** 155-166 (1989).
- [63] E. Flenner and G. Szamel, Nat. Comm. **6**, 7392 (2015).